Indian Journal of Geo Marine Sciences
Vol. 51 (02), February 2022, pp. 126-137

# Antiproliferative potential of *Sargassum binderi* Sonder ex J. Agardh mediated biogenic silver/silver chloride nanoparticles on EAC, MCF-7 and HCT116 cells

M S Ahamed, M M Rahman, I Hasan, S R Kabir & A K M Asaduzzaman*

[a]Department of Biochemistry and Molecular Biology, Faculty of Science, University of Rajshahi, Rajshahi – 6205, Bangladesh

*[E-mail: jonyasad2005@yahoo.com; jonyasad2005@ru.ac.bd]

*Received 04 August 2020; revised 15 January 2022*

Biosynthesis of Ag/AgCl-NPs from *Sargassum binderi* extract was confirmed by colour changes and a sharp peak at 416 nm detected by UV-visible spectrophotometer. It was characterized by Transmission Electron Microscopy (TEM), Energy Dispersive X-ray (EDX) spectrophotometer, X-ray powder Diffraction (XRD) and Fourier-Transform Infrared Spectroscopy (FTIR). Mild toxicity of the synthesized Ag/AgCl-NPs was determined by the brine shrimp nauplii cytotoxicity assay. $IC_{50}$ values of 19.73, 25.56, and 14.00 $\mu$g/ml showed the growth inhibition of Ehrlich Ascites Carcinoma (EAC), human breast cancer (MCF-7) and human colon cancer (HCT116) cells by Ag/AgCl-NPs, respectively. By analyzing cell morphological study using annexin V and caspase-3 inhibitor, initiation of apoptosis in EAC cells was confirmed. The results were further supported through the expression of several genes, where, *p53* and *Bax* genes became activated and *Bcl-X* and *NFκB* genes were suppressed.

[**Keywords**: Ag/AgCl-NPs, Apoptosis, Cancer cell inhibition, Gene expression, *Sargassum binderi*]

## Introduction

Seaweeds possess several bioactive substances like peptides, omega-3 fatty acids, laminarin, fucoidan, fucoxanthin, phlorotannin, etc., which have been employed as alternate medicines for a long time. They are used as delicious and popular food products in China, Japan, Korea and Thailand; in cosmetic industries; for animal feed additives and in freshwater treatment[1]. *Sargassum binderi*, a marine brown alga, contains plenty of bioactive compounds and its cultivation has already been started in Cox's Bazar region of Bangladesh. In the previous study, *S. binderi* extract was reported to contain huge amounts of phenolics, flavonoids and other phytoconstituents[2].

As an alternative anti-cancer agent, the importance of metal nanoparticles is significantly enhanced in the biomedical and pharmaceutical areas. Most effective nanoparticles are made from silver, gold and platinum. Among those, silver nanoparticles (AgNPs) have attracted many researchers due to their sterilized nature and marvellous medicinal worth. It is well-known that silver is safe for human cells at lower concentrations, while its toxic effects in microorganisms have also been reported[3].

Generally, traditional methods (biological, chemical and physical) are used for the synthesis of AgNPs. Among them, chemical and physical methods are costly and time-consuming. They also require reducing agents such as chemicals which pose an environmental burden. Hence, the green synthesis of AgNPs is of paramount importance to researchers because of its eco-friendliness and rapid production. Biological methods of synthesis of AgNPs include the utilization of plant extracts and microorganisms (bacteria and fungi). No specific culture media and culture conditions are needed for the synthesis of plant extract mediated AgNPs. Therefore, it is a more rapid, cheaper and eco-friendly method. Furthermore, plant-derived synthesis of AgNPs does not produce any toxic byproducts. In plants, various bioactive molecules are present that participate in the formation of AgNPs.

Now a day, cancer outbreaks are drastically elevating in the world and around 70 % of cancer deaths are reported from Africa, Asia, Central and South America[4]. So, researchers are aiming to decipher a potential drug for the effective treatment of cancer. AgNPs have potential anticancer properties and the growth of EAC, L929, Hep2, DLA, HT29 and MCF-7 cells was dose-dependently inhibited by AgNPs[5-8]. Plants, marine organisms and microbes are good natural resources and 60 % of the anticancer drugs were invented using these natural resources[9,10]. Compared to synthetic drugs, a natural product

originated drugs act more precisely and have lesser side effects[11].

Sea resources have a significant feature as anticarcinogenic agents. Many reports indicate different varieties of seaweeds as potential sources for the synthesis of AgNPs with anticarcinogenic properties[12,13]. As per literature review, *S. binderi* mediated Ag/AgCl-NPs with anticarcinogenic properties is not reported in the literature yet. Hence, the main aim of this work is to study the antitumor properties of *S. binderi* mediated Ag/AgCl-NPs and to check its potential as an anticarcinogenic drug.

## Materials and Methods

**Sample preparation**

Seaweed (*Sargassum binderi*) samples were collected from Cox's Bazar, Bangladesh. After washing with tap water and sun-drying, the samples were converted in to powder using a blender machine. The powder was then homogenized with distilled water at a ratio of 1:100 (w/v) for 15 min at 80 °C. After filtering the homogenate twice through a muslin cloth, the filtrate was centrifuged at 6,000 rpm for 15 min to obtain a light red coloured supernatant (*S. binderi* extract) which was stored at 4 °C for further analysis.

**Synthesis of Ag/AgCl-NPs**

The silver nitrate solutions of different concentrations (1.0, 2.0 and 3.0 mM) were prepared and mixed with *S. binderi* extract at 1:1 ratio (v/v). The solution was kept at room temperature for different reaction times (6 h, 12 h and 18 h) to complete the reaction and synthesize Ag/AgCl-NPs.

**Analysis of UV-visible spectra**

0.2 ml of the solution was mixed with 2 ml of deionized water and absorbance was recorded by UV-visible spectroscopy (Shimadzu, Japan) where the wavelength ranged from 750 to 250 nm. The reaction solution showing a sharp peak was centrifuged at 12,000 rpm for 10 min. The obtained precipitate was resuspended in deionized water and re-centrifuged. This step was repeated thrice and the sample was kept at 4 °C. After that, the re-dispersed solution was dried with a freeze dryer (Titec VD-800F, Japan) and the dried sample was used for further characterization.

**Transmission Electron Microscopy (TEM) analysis**

To determine the different sizes and shapes of the synthesized Ag/AgCl-NPs, TEM (JEM-2100F, JEOL, Japan) and the 'ImageJ' software program was used.

**Energy Dispersive X-ray spectroscopy (EDX) analysis**

Different atoms in synthesized Ag/AgCl-NPs were identified by EDX (JEM-2100F, JEOL, Japan) that was connected to the TEM.

**X-ray powder Diffraction (XRD) analysis**

For the XRD analysis, Ultima IV (Rigaku, Japan), an X-ray diffractometer with $CuK_{\alpha}1$ radiation was operated at 40 kV and 40 mA at a 2θ angle pattern.

**Fourier Transform Infrared Spectroscopy (FTIR) analysis**

Functional groups in synthesized Ag/AgCl-NPs were identified by using an FTIR (Perkin Elmer, USA) where the frequency ranges from 4000 – 225 $cm^{-1}$.

**Brine shrimp nauplii lethality assay**

Brine shrimp nauplii (*Artemia salina* L) lethality assay was performed following the method by Kabir *et al.*[14]. Ten nauplii were taken in each vial containing 4 ml of prepared sea water. Next, 10 – 160 µg/ml of *S. binderi* mediated Ag/AgCl-NPs were mixed to the vials. The experiment was done thrice at 30 °C for 24 h with a permanent light supply. After completing the experiment, mortality percentages of the nauplii were computed as well as $LC_{50}$ value was determined according to the method by Finney[15].

**EAC cells growth inhibition assay**

Growth inhibition of EAC cells was performed *in-vitro* according to the method by Kabir *et al.*[16]. At first, 100 µl of RPMI-1640 media was taken in a 96-well flat-bottom titer plate and 4 – 64 µg/ml of Ag/AgCl-NPs was added to its wells. Wells without NPs were used as controls. Finally, 100 µl of EAC cells ($5\times10^5$ cells/well) were added to each well and kept for incubation in a 5 % $CO_2$ incubator at 37 °C for 24 h. After completing the reaction, the aliquot was removed from each well followed by adding of 180 µl of PBS and 5 mg/ml of 20 µl of MTT and then kept in the incubator at 37 °C for overnight. After removing the aliquot from each well, 200 µl of acidic isopropanol was added and absorbance values were taken at 570 nm for each well using a titer plate reader.

**Cell culture**

DMEM medium was used to grow the MCF-7 cells in T25 cell culture flasks. Besides, 10 % FBS and 100 U/mL Neomycin and Streptomycin (NS) were added to the medium and kept at 37 °C in a 5 % $CO_2$ incubator. Subsequently, sub-cultures were done when confluence of the media reached 80 – 90 %.

**Growth inhibition assay of MCF-7 and HCT116 cells**

For *in-vitro* MCF-7 and HCT116 cell growth inhibition assay, 150 µl of MCF-7 and HCT116 cells ($2\times10^4$ cells/well) in DMEM medium (Gibco, USA) was added to a 96-well flat-bottom cell culture plate and kept for 24 h in a 5 % $CO_2$ incubator at 37 °C. After that, 50 µl of DMEM medium containing 4 – 64 µg/ml of Ag/AgCl-NPs was added in the wells to incubate for 48 h in the $CO_2$ incubator at 37 °C. Untreated MCF-7 and HCT116 cells were used as positive controls. Afterwards, 10 µl of tetrazolium compound [3-(4,5-dimethylthiazol-2-yl)-5-(3-carboxymethoxy phenyl)-2-(4-sulfophenyl)-2H-tetrazolium, inner salt; MTS(a)] with PES (phenazine ethosulfate) was added to each well and the plate was incubated in a 5% $CO_2$ incubator at 37 °C for 4 h. Finally, absorbance was recorded at 570 nm for each well by a titer plate reader and calculated cell proliferation inhibition by the following equation.

$$\text{Proliferation inhibition ratio (\%)} = (A-B)\times100/A$$

Where, A is the $OD_{570}$ nm of the cellular homogenate (control) without AgNPs and B is the $OD_{570}$ nm of the cellular homogenate with AgNPs.

**Morphological study of EAC cells by annexin V**

For the morphological study, untreated EAC cells (control) and *S. binderi* mediated Ag/AgCl-NPs-treated EAC cells were used. Cells were then kept warm in the 5 % $CO_2$ incubator at 37 °C for 24 h. Afterwards, EAC cells were washed with 10 mM Phosphate Buffer Saline (PBS). Then the cells were re-washed by using 1X supplied binding buffer. After that, annexin-V was used for staining cells and kept at room temperature in darkness for 20 min. Aliquots were removed from both EAC cells and washed by 1X binding buffer and finally, the morphology of cells was detected by optical and fluorescence microscope (Olympus iX71, Korea).

**Caspase-3 involvement assay**

The cell death assay was carried out to check the involvement of caspase-3 according to the Bio Vision manufacturer's guidelines. At first, 2 µmol/ml of caspase-3 inhibitor (z-DEVD-fmk) was mixed with EAC cells in RPMI-1640 media. Control cells were free of the inhibitor. Later on, cells were incubated in a 5 % $CO_2$ incubator at 37 °C for 2 h[ref. 17]. 64 µg/ml of Ag/AgCl-NPs was added to the caspase-3 inhibitor-treated and untreated EAC cells. The plate was incubated in the $CO_2$ incubator at 37 °C for 24 h. Untreated EAC cells in RPMI-1640 medium were used as control. Finally, an MTT assay was employed for the determination of cell growth inhibition.

**RNA isolation and gene expression**

For isolation of RNA and expression of genes, EAC cells were treated with 64 µg/ml of Ag/AgCl-NPs for 24 h. In accordance with the manufacturer's guidelines, RNA was separated from the treated and untreated EAC cells using TIANGEN BIOTECH reagent kit (Beijing, China). For RNA concentration and purity measurement, readings were taken at 260 nm and 280 nm. 1.5 % agarose gel electrophoresis was used to visualize the RNAs with a gel documentation system (Cleaver Scientific Ltd, DI-HD, UK). cDNA was synthesized with the help of a mixture of RT enzyme and RT buffer (Applied Biosystems, USA) with RNA. The primer sequences used for PCR reaction are provided in Table 1.

The PCR program was set in a thermal cycler (Gene, Atlas 482, Japan) for amplification as 95 °C for 3 min, 94 °C for 30 s, 55 °C for 30 s and 72 °C for 50 s for 40 cycles and 72 °C for 10 min. After completing the reaction, the product was kept on ice for 1 h and finally, it was kept at -20 °C until further use. 1.5 % agarose gel was used to visualize the gene expression of all the PCR products. 100 bp DNA ladder was used to compare with the standard.

Table 1 — List of primers

| Primer | Forward | Reverse |
|---|---|---|
| GAPDH | GTGGAAGGACTCATGACCACAG | CTGGTGCTCAGTGTAGCCCAG |
| p53 | GCGTCTTAGAGACAGTTGCCT | GGATAGGTCGGCGGTTCATGC |
| Bcl-X | TTGGACAATGGACTGGTTGA | GTAGAGTGGATGGTCAGTG |
| Bax | GGCCCACCAGCTCTGAGCAGA | GCCACGTGGGCGTCCCAAAGT |
| NFκB | AACAAAATGCCCCACGGTTA | GGGACGATGCAATGGACTGT |

**Statistical analysis**

All experiments were repeated thrice. Data were expressed as the mean ± SD; where, $P < 0.05$. To analyze the data by one way ANOVA using Dunnett's test, SPSS software version 16 (SPSS Inc., Chicago, IL, USA) was used.

## Results

**Ag/AgCl-NPs synthesis**

The light red colour of *S. binderi* extract solution slowly turned to the dark brown colour upon completion of the reaction as described above in the methodology in 6, 12 and 18 h indicating the formation of Ag/AgCl nanoparticles.

**UV-visible spectra for Ag/AgCl-NPs synthesis**

A sharp peak of synthesized Ag/AgCl-NPs was observed at 416 nm using 1.0 mM of $AgNO_3$ for 18 h (Fig. 1a – c).

**Analysis by TEM**

Highly monodispersed cubic shaped Ag/AgCl-NPs were found in TEM analysis (Fig. 2a). Figure 2(b) showed an average particle size of 29 nm.

**EDX analysis**

*S. binderi* extract mediated silver nanoparticles produced a signal revealing the existence of Ag in the synthesized nanoparticles (Fig. 2c). The presence of the strong signals from carbon (43.86 %) and silver (41.06 %) atoms and weak signals from the chlorine (15.07 %) atom in nanoparticles was confirmed.

**XRD analysis**

According to the crystallographic planes (111, 200, 220, 311 and 222), the XRD reflection peaks were monitored at 27.7°, 32.12°, 46.06°, 54.74° and 57.36°, respectively which confirmed the formation of AgCl-NPs (JCPDS card no. 31-1238). Corresponding to planes (111, 200 and 220), reflection peaks were observed at 38.08°, 44.21° and 64.46°, respectively for AgNPs (JCPDS card no. 65-2871) (Fig. 2d).

**FTIR analysis**

In FTIR analysis, different major peaks were obtained in *S. binderi* extract and synthesized nanoparticles (Fig. 3a, b). The main peaks in *S. binderi* extract were 3435.46, 1638.92, 1384.28, 1129.08, 928.71, 848.56 and 615.87 $cm^{-1}$. On the contrary, peaks at 3413.01, 2920.61, 1384.17 and 1068.64 $cm^{-1}$ were observed in synthesized Ag/AgCl-NPs.

**Toxicity**

Brine shrimp nauplii toxicity assay was performed to predict the toxicity of synthesized Ag/AgCl-NPs. 23.33 % to 80 % of brine shrimp nauplii mortality was observed by using 10 to 160 µg/ml of Ag/AgCl-NPs. The mortality rate increased with the increase in concentration of Ag/AgCl-NPs (Fig. 4). The $LC_{50}$ value of Ag/AgCl-NPs was 60.14 µg/ml.

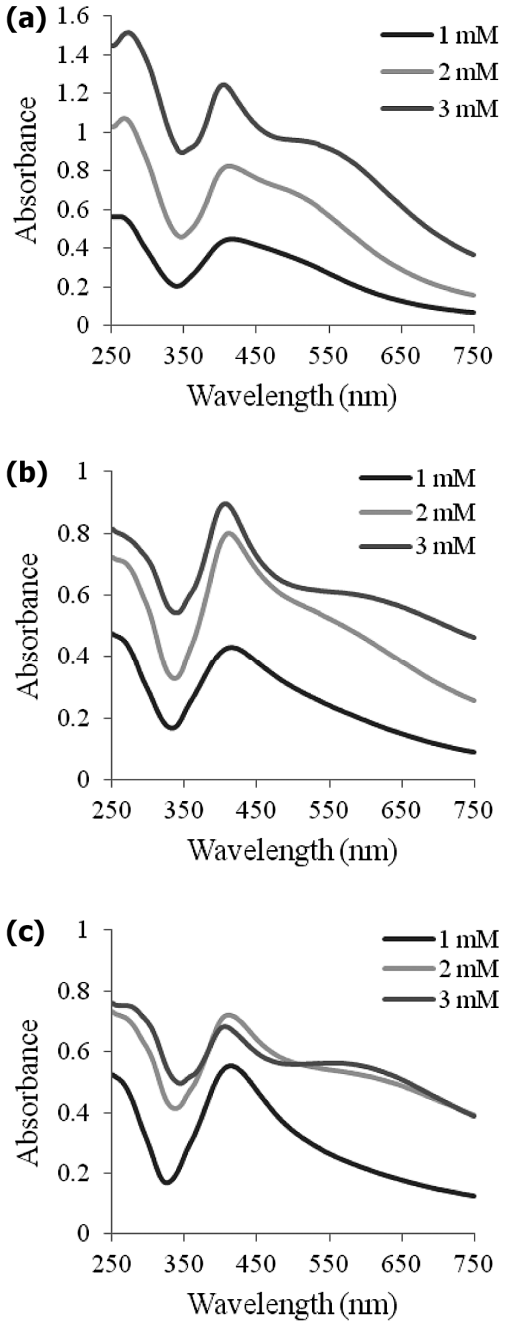


Fig. 1 — UV-visible spectra of *S. binderi* mediated Ag/AgCl-NPs using different time (h) for reaction: (a) 6 h; (b) 12 h; and (c) 18 h

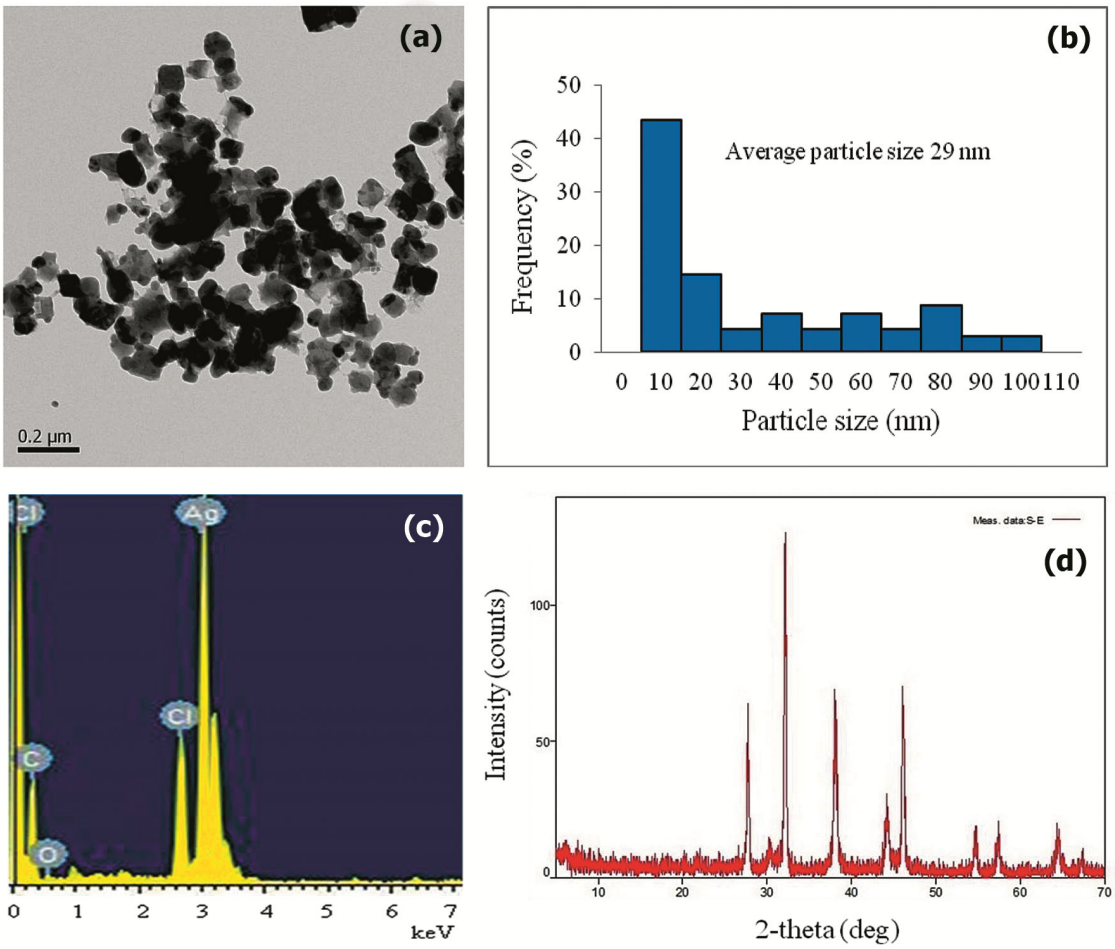


Fig. 2 — (a) TEM images of *S. binderi* mediated Ag/AgCl-NPs; (b) Percentage of different sizes *S. binderi* mediated Ag/AgCl-NPs; (c) EDX spectra of *S. binderi* mediated AgNPs; and (d) X-Ray Diffraction (XRD) pattern of synthesized silver nanoparticles

**Antiproliferative activity of Ag/AgCl-NPs on EAC, MCF-7 and HCT116 cells**

MTT assay was performed to recognize the antiproliferative potential of Ag/AgCl-NPs against the EAC cells. 87.38 % of EAC cells growth inhibition was observed at 64 $\mu$g/ml of Ag/AgCl-NPs. Inhibition of EAC cell growth was also decreased dose-specifically with reducing concentrations of Ag/AgCl-NPs, as shown in Figure 5(a). However, 86.75 % and 90.08 % of MCF-7 and HCT116 cells growth inhibition were detected at 64 and 32 $\mu$g/ml, respectively which was also dose-specific (Fig. 5b, c). The $IC_{50}$ value of synthesized Ag/AgCl-NPs on EAC cells was calculated as 19.73 $\mu$g/ml, whereas $IC_{50}$ values obtained for MCF-7 and HCT116 cells were 25.56 $\mu$g/ml and 14.00 $\mu$g/ml, respectively.

**Cell morphological examination**

For cell morphological examination, an optical and fluorescence microscope was used. By using an optical microscope, round-shaped untreated EAC cells were seen whereas morphological alteration of cells was observed in Ag/AgCl-NPs-treated EAC cells (Fig. 6a & b). No green colour around the untreated EAC cell surface was detected by fluorescence microscope (Fig. 6c, e). However, EAC cells treated with Ag/AgCl-NPs exhibited a green colour image (Fig. 6d, f) suggesting the occurrence of apoptosis in those cells.

**Effect of caspase-3 inhibitor on EAC cells treated with *S. binderi* mediated Ag/AgCl-NPs**

Ag/AgCl-NPs induced cell death assay was performed to check the role of caspase-3, using a caspase-3 inhibitor (z-DEVD-fmk). *S. binderi* mediated Ag/AgCl-NPs induced 87.38 % cell growth inhibition at 64 µg/ml, whereas the cell growth was reduced to 31.04 % along with caspase-3 inhibitor but there was no effect on cell growth inhibition when only caspase-3 inhibitor was used (Fig. 7).

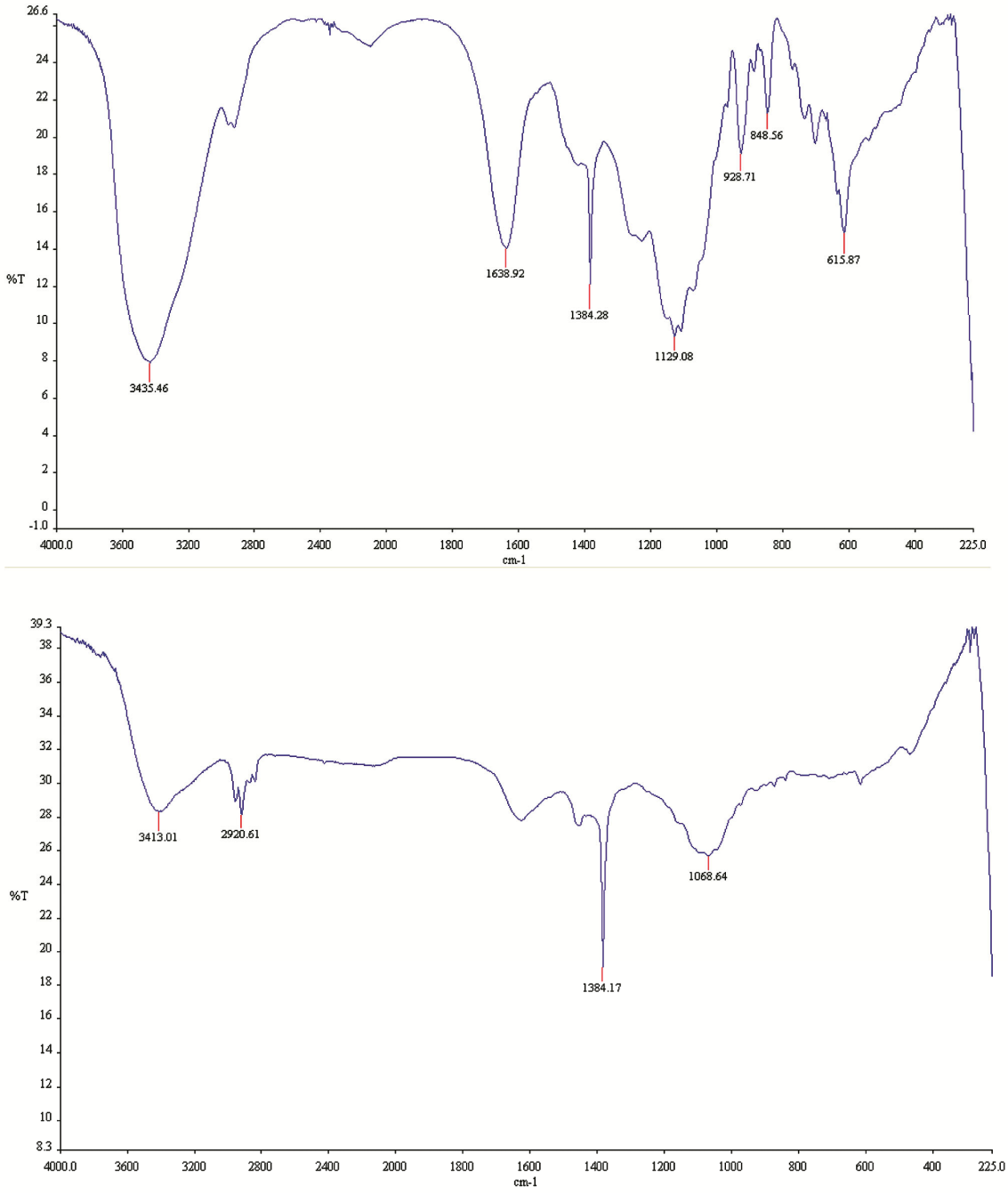


Fig. 3 — (a) FTIR spectrum of *S. binderi* extract, and (b) *S. binderi* mediated Ag/AgCl-NPs

**Apoptosis-related gene expression**

In this study, *p53* and *Bax* gene expression was noticed in EAC cells treated with Ag/AgCl-NPs, though the expression of *Bcl-X* gene was not present. Opposite expression of the corresponding genes was found in the control EAC cells (not treated with Ag/AgCl-NPs). In both conditions, *GAPDH* gene expression was seen. *NFκB* gene expression in treated EAC cells got reduced as compared to the untreated cells (Fig. 8).

## Discussion

Recently, the importance of AgNPs has drastically increased in the pharmaceutical and medical fields due to their negligible toxicity to the normal cells[18]. In this study, the formation of AgNPs was detected by

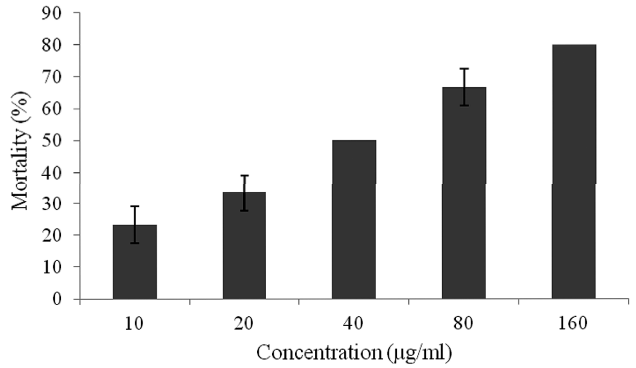


Fig. 4 — Mortality rate of brine shrimp nauplii using the treatment of *S. binderi* mediated Ag/AgCl-NPs (n = 3, mean ± S.D.; $P < 0.05$)

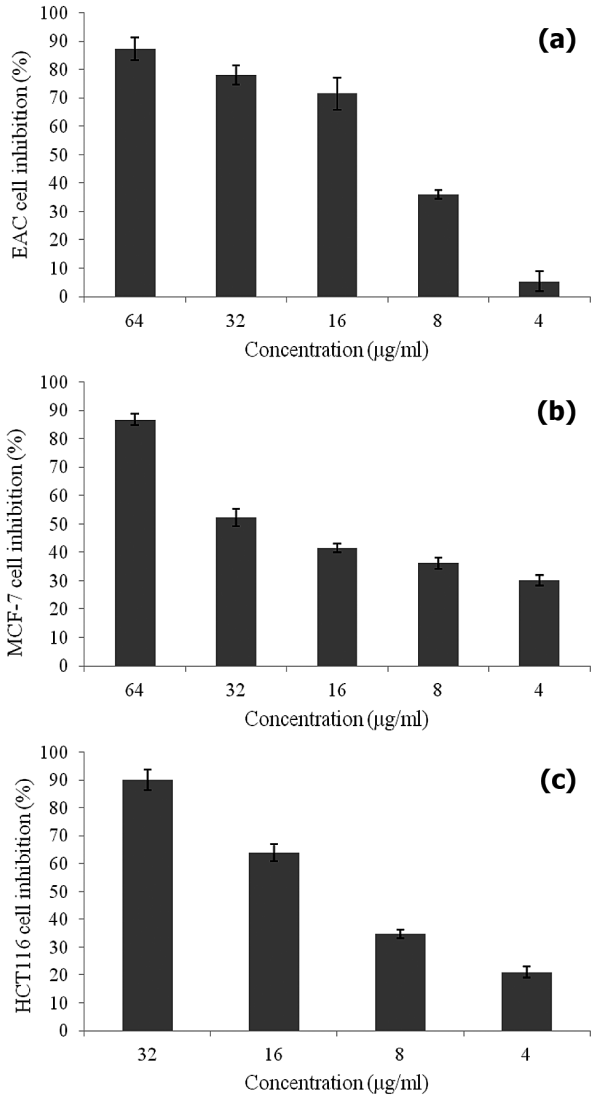


Fig. 5 — Inhibition of (a) EAC, and (b) MCF-7 cell growth by the treatment of *S. binderi* mediated Ag/AgCl-NPs (n = 3, mean ± S.D.; $P < 0.05$).

the conversion of a light reddish coloured solution of *S. binderi* extract to a dark brown coloured solution. It might have happened due to the reduction of $AgNO_3$ by the bioactive compounds present in the aqueous solution of *S. binderi* extract. Generally, an absorption peak of AgNPs appears at the UV-visible range of 380 – 450 nm due to their size reliant properties[19]. In this study, an SPR peak at 416 nm was detected. Similar data were reported for aqueous extract of *Ecklonia cava* by Jayachandran *et al.*[20] who found a strong SPR peak at 418 nm confirming the formation of AgNPs. Further, an SPR peak of at 408 nm was reported by Mohandass *et al.*[21] in *S. cinereum* extract assisted with AgNPs.

Moreover, AgNPs have significant physicochemical uniqueness due to their shape, size, solubility and surface charge. Therefore, they can demonstrate key functions for determining biological reactions. In the present study, the synthesized Ag/AgCl-NPs were cubic-shaped. The middling particle size of *S. binderi* mediated Ag/AgCl-NPs was around 29 nm which was in line with the earlier reports on *Ecklonia cava* extract assisted AgNPs[20]. After EDX analysis of *S. binderi* mediated Ag/AgCl-NPs, an absorption peak for elemental Ag was noticed in the range of 3 to 4 keV. Similar results were also seen by Magudapathy *et al.*[22]. Weaker peaks for Cl and C were present in the EDX spectra as seaweeds contain some bioactive compounds such as phenolic, flavonoid, protein and polysaccaharides which are released by X-ray emission[23]. The crystalline nature of Ag/AgCl-NPs was confirmed by its XRD spectra. At the first stage of the reaction process, AgCl is formed by $Ag^+$ from $AgNO_3$ and $Cl^-$ from the phytochemical compounds of *S. binderi* extract. During the formation of AgCl, these phytochemical compounds also acted as reducing agents to reduce $Ag^+$ to metallic Ag. Later, $Ag^+$ formed an intermediate complex with OH groups of phenolic and flavonoid compounds originating from the extract. This intermediate complex went through an oxidation reaction to reduce $Ag^+$ to AgNPs. A similar observation was also made by Okaiyeto *et al.*[24].

To identify FT-IR bands in synthesized Ag/AgCl-NPs tentatively, standard FTIR spectra[25,26] was used. Significant changes in FTIR peak were found in *S. binderi* extract mediated Ag/AgCl-NPs compared to the control extract. The changed peak at 3413.01 $cm^{-1}$ in Ag/AgCl-NPs was hydroxyl (-OH) functional group in phenolic and flavonoid compounds that

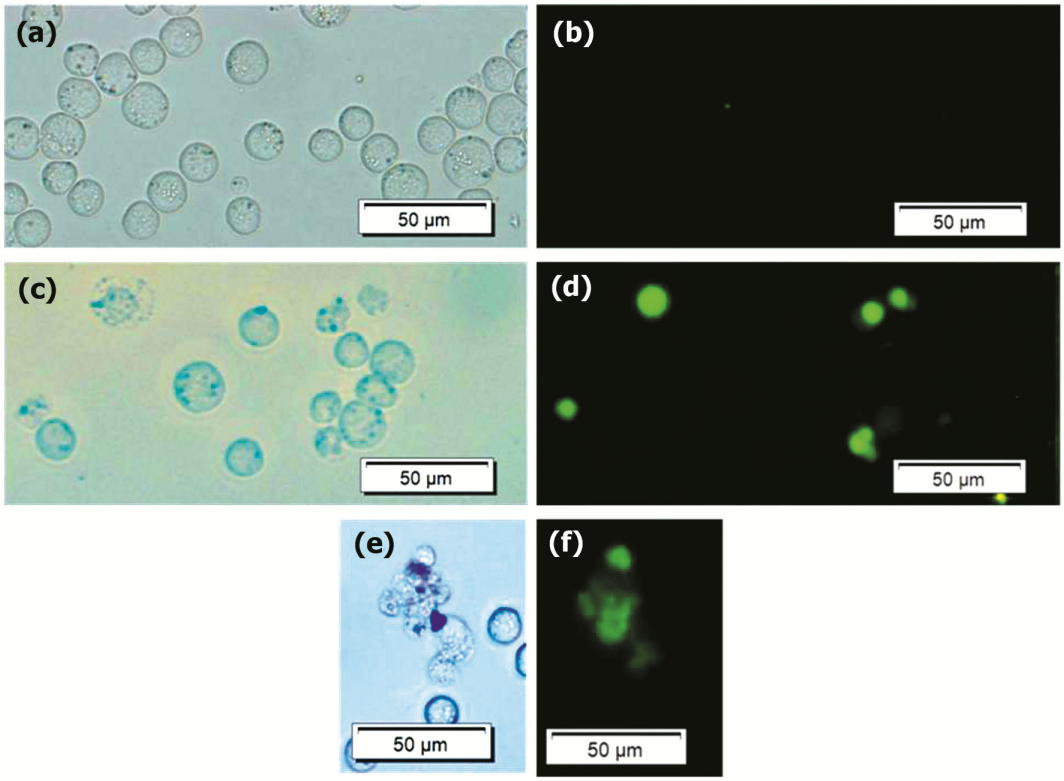


Fig. 6 — Morphological alteration in EAC cells treated with and without Ag/AgCl-NPs: a - (optical) and b - (fluorescence) are untreated EAC cells whereas, c & e (optical) and d & f (fluorescence) are Ag/AgCl-NPs treated EAC cells

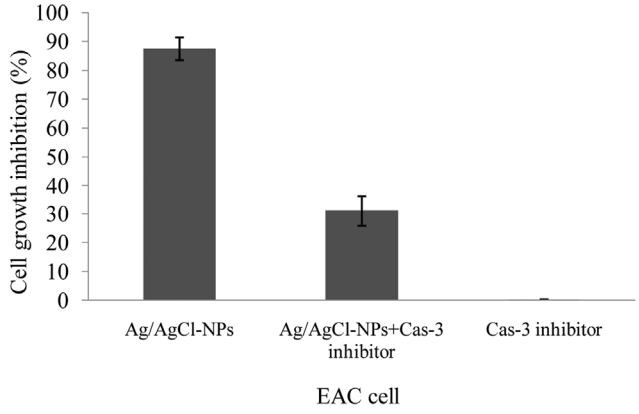


Fig. 7 — Inhibition of EAC cells growth by the treatment of *S. binderi* mediated Ag/AgCl-NPs with caspase-3 inhibitor (n = 3, mean ± S.D.; $P < 0.05$)

might be used for the reduction of $Ag^+$ to AgNPs[27,28]. Another small peak was at 2920.61 $cm^{-1}$ in Ag/AgCl-NPs that might be carbonyl groups and secondary amines. However, the peak at 1384.17 $cm^{-1}$ was a stretching for (N-O) functional group and 1068.64 $cm^{-1}$ in Ag/AgCl-NPs, there was possibly a carbonyl (C=O) functional group. The modified peak in hydroxyl and carbonyl groups in FTIR spectra of

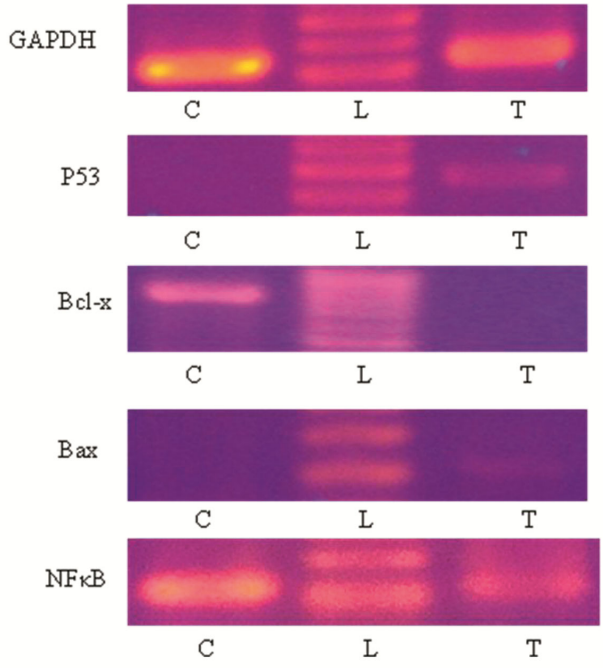


Fig. 8 — Investigation of GAPH, *p53*, *Bax*, *Bcl-x* and *NFκB* genes expression in EAC cells treated with and without Ag/AgCl-NPs. L - 100 bp DNA ladder; T - Ag/AgCl-NPs treated EAC cells; | C - untreated EAC cells or control

AgNPs authenticated the oxidation of amines, phenols, flavonols, amides and other secondary metabolites of the seaweed extract[29]. It was also noticed that the synthesized Ag/AgCl-NPs were surrounded by bioactive molecules existing in the extract. Proteins or amino acids contain carbonyl groups that have a well-built aptitude to attach with metals as capping agents so that the Ag/AgCl-NPs are stabilized. As a whole, it can be said that bioactive molecules from plant extract can act both for synthesis and stabilization of Ag/AgCl-NPs[30]. Another researcher reported that amines or cysteine residues in proteins may also act for the stabilization of AgNPs[31].

In the brine shrimp nauplii cytotoxicity assay, $LC_{50}$ value of *S. binderi* mediated Ag/AgCl-NPs was 60.14 µg/ml. Compared to the present study, $LC_{50}$ value of *Bergenia ciliate* mediated AgNPs (32.92 µg/ml) was lower and $LC_{50}$ value of *Turbinaria conoides* mediated AgNPs (88.91 µg/ml) was higher[32,33]. From the above results, it can be concluded that *S. binderi* mediated biogenic Ag/AgCl-NPs have potential effects that are moderately toxic for living animals.

It became evident that all types of seaweeds include numerous bioactive compounds that have important therapeutic values. Some of these bioactive compounds are useful to develop novel drugs against cancer. A number of biosynthesized secondary metabolites from marine plants with antitumor property have been reported earlier[34]. In general, cancer is termed as an uncontrolled growth of cells. Cancer remains the most important cause of death that keeps rising in the last few years[35]. In this study, the EAC, MCF-7 and HCT116 cells were used to evaluate the toxicity of *S. binderi* mediated Ag/AgCl-NPs. Nearly 87.38 %, 86.75 % and 90.08 % of growth inhibition was observed against EAC, MCF-7 and HCT116 cells with doses of 64, 64 and 32 µg/ml, respectively. Other researchers reported that 94 % and 99 % of EAC cell growth inhibition were observed by *Ulva fasciata* and *Turbinaria turbinata* mediated AgNPs at 98 µg/ml[36]. Different levels of anticancer activity of plant seaweed extract mediated Ag/AgCl-NPs against different cancer cell lines were observed. $IC_{50}$ value of *S. binderi* mediated Ag/AgCl-NPs on MCF-7 and HCT116 cells were 25.56 and 14.00 µg/ml. Comparable results have been obtained in HeLa cells where $IC_{50}$ value of *Podophyllum hexandrum* and *Cymodocea serrulata* mediated AgNPs was 20 and 34.5 µg/ml, respectively[37,38]. Significant inhibition of the proliferation of Hep2 and MCF7 cells by *Ulva lactuca* seaweed assisted AgNPs was found with $IC_{50}$ values of 12.5 and 37 µg/ml[6]. $IC_{50}$ value of *Oscillatoria limnetica* mediated AgNPs was 5.369 against HCT116 cells whereas that of GM mediated AgNPs was 40.2 µg/ml[39,40].

Most cellular deaths occur through apoptosis and autophagy. Many changes are observed in cells during apoptosis such as cell shrinkage, condensation of chromatins, fragmentation of nucleus and DNA as well as formation of the apoptotic bodies. Different types of caspase-mediated cell death occur by morphological changes. For anticancer drug discovery, finding an agent causing apoptosis in cancer cells is attractive for the researchers.

In this study, morphological changes that occur in Ag/AgCl-NPs treated EAC cells were assured by optical microscope as well as by fluorescence microscope as green colour indicating apoptotic cell death. Generally, caspase-3 inhibitor obstructs the binding sites on caspase-3. Therefore, caspase-3 inhibitor in Ag/AgCl-NPs treated EAC cells was used to reduce the protein activation. Cell growth inhibition became significantly reduced showing the association of a caspase-3 reliant alleyway. Different cancer cells induced apoptosis by the use of plant-mediated AgNPs. A *Padina tetrastromatica* mediated AgNPs and *Artemisia turcomanica* leaf extract mediated AgNPs reduced the growth of MCF-7 and AGS cell lines by inducing apoptosis following caspase-dependent pathways[41,42].

It is now well established that, many genes are also included in any apoptosis reliant alleyway. Generally, it is known that *Bax*, *Bid* and *Bak* genes are included in the pro-apoptotic classes as well as *NFκB* and *Bcl-X* are anti-apoptotic classes. For apoptotic cell death, *Bcl-X* gene is replaced by *Bax*, *Bak* and *Bid* genes. *p53* is an important gene for apoptosis modulator followed by DNA damage, cell cycle arrest and binding with *Bcl-X* protein. Therefore, *Bax* gene can give a signal to the mitochondria for cell death[43]. However, *NFκB* is a transcription factor involved in cancer cell proliferation[44]. In this study, *Bcl-X* gene became activated in control EAC cells but in the case of EAC cells treated with *S. binderi* mediated Ag/AgCl-NPs, it became deactivated. However, *p53* and *Bax* genes were activated in Ag/AgCl-NPs

treated EAC cells but not in control EAC cells. *NF-κB* gene also showed this trend. Starch mediated AgNPs also showed similar reports in human colon cancer cells[9]. Groc *et al.*[45] reported that activated *Bcl-X* blocked apoptotic processes by the prevention of cytochrome-c translocation whereas activated *Bax* and *Bak* did not block apoptosis[45]. As a whole, it can be said that *S. binderi* mediated biogenic AgNPs caused apoptosis in EAC cells through the activation of *p53* and *Bax* genes with an inhibited expression of *NF-κB*.

## Conclusion

In brief, the successful synthesis of Ag/AgCl-NPs from *S. binderi* extract cultivated from Bangladesh which was cubic shaped is presented here. Synthesized Ag/AgCl-NPs have significant anticancer activity against EAC, MCF-7 and HCT116 cells. The potent anticancer property against EAC cells might be used to design an anticancer drug in future.

## Acknowledgements

This research was financed by the Faculty of Science, University of Rajshahi, Bangladesh, No. A-54-5/52/RU/Science-11/17-18.

## Conflict of Interests

Authors of this manuscript declares no conflict of interest.

## Author Contributions

The following authors contributed to the successful completion of this article.MSA & MMR: Research experiment; IH: Research experiment, helping article reviewing and funding; SRK: Research experiment and helping article reviewing; AKMA: Idea generation, research experiment, article writing, supervision and funding.

## References

1 Wang W L & Chiang Y M, Potential economic seaweeds of *Hengchum peninsula*, Taiwan, *Econ Bot*, 84 (2) (1994) 182–189.

2 Asaduzzaman A K M, Hasan I, Rahman M H & Tareq A R M, Antioxidant and antiproliferative activity of phytoconstituents identified from *Sargassum binderi* seaweed extracts cultivated in Bangladesh, *Int J Biosci*, 16 (3) (2020) 481–494.

3 Mollick M M R, Rana D, Dash S K, Chattopadhyay S, Bhowmick B, *et al.*, Studies on green synthesized silver nanoparticles using *Abelmoschus esculentus* (L.) pulp extract having anticancer (*in vitro*) and antimicrobial applications, *Arabian J Chem*, 12 (8) (2019) 2572–2584. https://doi.org/10.1016/j.arabjc.2015.04.033

4 Stewart B W & Wild C P, *World Cancer Report*, (International Agency for Research on Cancer, Lyon, France), 2014, pp. 1-630.

5 Nallathamby P D & Xu X H, Study of cytotoxic and therapeutic effects of stable and purified silver nanoparticles on tumor cells, *Nanoscale*, 2 (6) (2010) 942–952.

6 Sriram M I, Kanth S B, Kalishwaralal K & Gurunathan S, Antitumor activity of silver nanoparticles in Dalton's lymphoma ascites tumor model, *Int J Nanomed*, 5 (2010) 753–762.

7 Devi J S & Bhimba B V, Anticancer activity of silver nanoparticles synthesized by the seaweed *Ulva lactuca* in vitro, *Sci Rep*, 1 (4) (2012) p. 242. doi:10.4172/scientificreports.242

8 Asaduzzaman A K M, Chun B S & Kabir S R, *Vitis vinifera* assisted silver nanoparticles with antibacterial and antiproliferative activity against Ehrlich ascites carcinoma cells, *J Nanoparticle*, (2016) p. 6898926. https://doi.org/10.1155/2016/6898926

9 Satapathy S R, Mohapatra P, Preet R, Das D, Sarkar B, *et al.*, Silver-based nanoparticles induce apoptosis in human colon cancer cells mediated through p53, *Nanomed*, 8 (8) (2013) 1307–1322.

10 Newman M J, Foster D L, Wilson T H & Kaback H R, Purification and reconstitution of functional lactose carrier from *Escherichia coli*, *J Biol Chem*, 256 (22) (1981) 11804–11808.

11 Paterson I & Anderson E A, The renaissance of natural products as drug candidates, *Science*, 310 (5747) (2005) 451–453.

12 Shanmugam N, Rajkamal P, Cholan S, Kannadasan N, Sathishkumar K, *et al.*, Biosynthesis of silver nanoparticles from the marine seaweed *Sargassum wightii* and their antibacterial activity against some human pathogens, *Appl Nanosci*, 4 (2014) 881–888.

13 Jayaprakash P, Sivakumari K, Ashok K, Rajesh S, Prabhu D, *et al.*, Anticancer potential of green synthesized silver nanoparticles of *Sargassum wightii* against human prostate cancer (pc-3) cell line, *Eur J Pharm Med Res*, 4 (3) (2017) 275–287.

14 Kabir S R, Hossen A, Zubair A, Alom J, Islam F, *et al.*, A new lectin from the tuberous rhizome of *Kaempferia rotunda*: isolation, characterization, antibacterial and antiproliferative activities, *Protein Pept Lett*, 18 (11) (2011) 1140–1149.

15 Finney D J, *Probit Analysis*, (Cambridge University press, London), (1971), pp. 333.

16 Kabir S R, Nabi M M, Haque A, Zaman R U, Mahmud Z H, *et al.*, Pea lectin inhibits growth of Ehrlich ascites carcinoma cells by inducing apoptosis and G2/M cell cycle arrest in vivo in mice, *Phytomed*, 20 (14) (2013) 1288–1296.

17 Lyu S Y, Park W B, Choi K H & Kim W H, Involvement of caspase-3 in apoptosis induced by *Viscum album* var. coloratum agglutinin in HL-60 cells, *Biosci Biotechnol Biochem*, 65 (3) (2001) 534–541.

18 Silver S, Bacterial silver resistance: molecular biology and uses and misuses of silver compounds, *FEMS Microbio Rev*, 27 (2-3) (2003) 341–353.

19 Duran N, Marcato P D, Alves O L, De Souza G I & Esposito E, Mechanistic aspects of biosynthesis of silver nanoparticles by several *Fusarium oxysporum* strains, *J Nanobiotechnol*, 3 (8) (2005) 1–7.

20 Venkatesan J, Kim S K & Shim M S, Antimicrobial, antioxidant, and anticancer activities of biosynthesized silver nanoparticles using marine algae *Ecklonia cava*, *Nanomaterials*, 6 (12) (2016) 235. https://doi.org/10.3390/nano6120235

21 Mohandass C, Vijayaraj A, Rajasabapathy R, Satheeshbabu S, Rao S, *et al.*, Biosynthesis of silver nanoparticles from marine seaweed *Sargassum cinereum* and their antibacterial activity, *Ind J Pharm Sci*, 75 (5) (2013) 606–610.

22 Magudapathy P, Gangopadhyay P, Panigrahi B K, Nair K G M & Dhara S, Electrical transport studies of Ag nanoclusters embedded in glass matrix, *Physica B*, 299 (1-2) (2001) 142–146.

23 Devi J S, Bhimba B V & Peter D M, Production of biogenic silver nanoparticles using *Sargassum longifolium* and its applications, *Indian J Geo-Mar Sci*, 42 (1) (2013) 125–130.

24 Okaiyeto K, Ojemaye M O, Hoppe H, Mabinya L V & Okoh A I, Phytofabrication of silver/silver chloride nanoparticles using aqueous leaf extract of *Oedera genistifolia*: characterization and antibacterial potential, *Molecule*, 24 (23) (2019) 4382. https://doi.org/10.3390/molecules24234382

25 Dean S A & Tobin J M, Uptake of chromium cations and anions by milled peat, *Resour Conserv Recycl*, 27 (1-2) (1999) 151–156.

26 Sigee D C, Dean A, Levado E & Tobin M J, Fourier-transform infrared spectroscopy of *Pediastrum duplex*: characterization of a micro-population isolated from a eutrophic lake, *Eur J Phycol*, 37 (2002) 19–26.

27 Elavazhagan T & Arunachalam K D, *Memecylon edule* leaf extract mediated green synthesis of silver and gold nanoparticles, *Int J Nanomed*, 6 (2011) 1265–1278. https://doi.org/10.2147/IJN.S18347

28 Geethalakshmi R & Sarada D V L, Gold and silver nanoparticles from *Trianthema decandra*: synthesis, characterization, and antimicrobial properties, *Int J Nanomed*, 7 (2012) 5375–5384. https://doi.org/10.2147/IJN.S36516

29 Merin D D, Prakash S & Bhimba V B, Antibacterial screening of silver nanoparticles synthesized by marine microalgae, *Asian Pacific J Tropical Med*, 3 (10) (2010) 797–798.

30 Krishnara C, Jagan E G, Rajasekhar S, Selvakumar P, Kalaichelvan P T, *et al.*, Synthesis of silver nanoparticles using *Acalypha indica* leaf extracts and its antibacterial activity against water borne pathogens, *Colloid Surf B Biointerf*, 76 (1) (2010) 50–56.

31 Gole A, Dash C, Ramakrishnan V, Sainkar S R, Mandale A B, *et al.*, Pepsin-gold colloid conjugates: preparation, characterization and enzymatic activity, *Langmuir*, 17 (5) (2001) 1674–1679.

32 Phull A R, Abbas Q, Ali A, Raza H, Kim S J, *et al.*, Antioxidant, cytotoxic and antimicrobial activities of green synthesized silver nanoparticles from crude extract of *Bergenia ciliate*, *Future J Pharm Sci*, 2 (1) (2016) 3 1–36.

33 Vijayan S R, Santhiyagu P, Singamuthu M, Kumari Ahila, N, Jayaraman R, *et al.*, Synthesis and characterization of silver and gold nanoparticles using aqueous extract of seaweed, *Turbinaria conoides*, and their antimicrofouling activity, *The Sci World J*, (2014) 938272. https://doi.org/10.1155/2014/938272

34 Manilal A, Sujith S, Kiran G S, Selvin J, Shakir C, *et al*., Bio-potentials of seaweeds collected from Southwest coast of India, *J Marine Sci Technol*, 17 (1) (2009) 67–73.

35 Xia M, Wang D & Wang M, Dracordohin perchlorate induces apoptosis via activation of caspase and generation of reactive oxygen species, *J Pharmacol Sci*, 95 (2) (2004) 278–283.

36 Khalifa K S, Hamouda R, Hanafy D & Hamza A, In vitro antitumor activity of silver nanoparticles biosynthesized by marine algae, *Digest J Nanomater Biostruct*, 11 (1) (2016) 213–221.

37 Jeyaraj M, Rajesh M, Arun R, Ali D M, Sathishkumar G, *et al.*, An investigation on the cytotoxicity and caspase-mediated apoptotic effect of biologically synthesized silver nanoparticles using *Podophyllum hexandrum* on human cervical carcinoma cells, *Colloid Surf B Biointerf*, 102 (2013) 708–717.

38 Chanthini A B, Balasubramani G, Ramkumar R, Sowmiya R, Balakumaran M D, *et al.*, Structural characterization, antioxidant and in vitro cytotoxic properties of seagrass, *Cymodocea serrulata* (R.Br.) Asch. & Magnus mediated silver nanoparticles, *J Photochem Photobiol B Biol*, 153 (2015) 145–152.

39 Hamouda R A, Hussein M H, Abo-elmagd R A & Bawazir S S, Synthesis and biological characterization of silver nanoparticles derived from the cyanobacterium *Oscillatoria limnetica*, *Sci Rep*, 9 (1) (2019) 13071. https://doi.org/10.1038/s41598-019-49444-y

40 Lee K X, Shameli K, Mohamad S E, Yew Y P, Isa E D M, *et al.*, Bio-Mediated synthesis and characterisation of silver nanocarrier, and its potent anticancer action, *Nanomaterials*, 9 (10) (2019) 1423. https://doi.org/10.3390/nano9101423

41 Selvi B C G, Madhavan J & Santhanam A, Cytotoxic effect of silver nanoparticles synthesized from *Padina tetrastromatica* on breast cancer cell line, *Adv Nat Sci Nanosci Nanotechnol*, 7 (3) (2016) 035015. doi:10.1088/2043-6262/7/3/035015.

42 Mousavi B, Tafvizi F & Bostanabad S Z, Green synthesis of silver nanoparticles using *Artemisia turcomanica* leaf extract and the study of anti-cancer effect and apoptosis induction on gastric cancer cell line (AGS), *Artif Cells Nanomed Biotechnol*, 46 (sup1) (2018) 499–510. https://doi.org/10.1080/21691401.2018.1430697

43 Yu J & Zhang L, PUMA, a potent killer with or without p53, *Oncogene*, 27 (1) (2008) 71–83.

44 Borner C, The Bcl-2 protein family: sensors and checkpoints for life-or death decisions, *Molecular Immunol*, 39 (11) (2003) 615–647.

45 Groc L, Bezin L, Jiang H, Jackson T S & Levine R A, Bax, Bcl-2, and cyclin expression and apoptosis in rat substantia nigra during development, *Neurosci Lett*, 306 (3) (2001) 198–202.